The Journal of Experimental Biology 203, 3585–3594 (2000)
Printed in Great Britain © The Company of Biologists Limited 2000
JEB3039



# FUNCTION OF THE HETEROCERCAL TAIL IN WHITE STURGEON: FLOW VISUALIZATION DURING STEADY SWIMMING AND VERTICAL MANEUVERING

JAMES LIAO* AND GEORGE V. LAUDER

*Department of Organismic and Evolutionary Biology, Harvard University, Cambridge, MA 02138, USA*

*Author for correspondence (e-mail: jliao@oeb.harvard.edu)

*Accepted 4 September; published on WWW 2 November 2000*

## Summary

**Basal ray-finned fishes possess a heterocercal tail in which the dorsal lobe containing the extension of the vertebral column is longer than the ventral lobe. Clarifying the function of the heterocercal tail has proved elusive because of the difficulty of measuring the direction of force produced relative to body position in the aquatic medium. We measured the direction of force produced by the heterocercal tail of the white sturgeon (*Acipenser transmontanus*) by visualizing flow in the wake of the tail using digital particle image velocimetry (DPIV) while simultaneously recording body position and motion using high-speed video. To quantify tail function, we measured the vertical body velocity, the body angle and the path angle of the body from video recordings and the vortex ring axis angle and vortex jet angle from DPIV recordings of the wake downstream from the tail. These variables were measured for sturgeon exhibiting three swimming behaviors at $1.2\,L\,s^{-1}$, where $L$ is total body length: rising through the water column, holding vertical position, and sinking through the water column. For vertical body velocity, body angle and path angle values, all behaviors were significantly different from one another. For vortex ring axis angle and vortex jet angle, rising and holding behavior were not significantly different from each other, but both were significantly different from sinking behavior. During steady horizontal swimming, the sturgeon tail generates a lift force relative to the path of motion but no rotational moment because the reaction force passes through the center of mass. For a rising sturgeon, the tail does not produce a lift force but causes the tail to rotate ventrally in relation to the head since the reaction force passes ventral to the center of mass. While sinking, the direction of the fluid jet produced by the tail relative to the path of motion causes a lift force to be created and causes the tail to rotate dorsally in relation to the head since the reaction force passes dorsal to the center of mass. These data provide evidence that sturgeon can actively control the direction of force produced by their tail while maneuvering through the water column because the relationship between vortex jet angle and body angle is not constant.**

Key words: locomotion, sturgeon, heterocercal tail, flow visualization, hydrodynamics, *Acipenser transmontanus*, force balance.

## Introduction

Most elasmobranchs and basal ray-finned fishes possess an asymmetrical tail morphology in which the dorsal lobe, containing the extension of the vertebral column, is longer than the ventral lobe. Over the last century, studies investigating the function of this plesiomorphic tail morphology have proposed that the movement of the heterocercal tail pushes water postero-ventrally, generating both thrust and lift (Grove and Newell, 1936; Affleck, 1950; Alexander, 1965; Simons, 1970; Olson, 1971; Ferry and Lauder, 1996). This classical model of heterocercal tail function asserts that the postero-ventrally directed force is generated by the stiffer upper lobe leading the lower lobe during the oscillatory cycle. Most recently, Ferry and Lauder (1996) used three-dimensional kinematics and dye-streams to confirm that the heterocercal tail of a freely swimming leopard shark (*Triakis semifasciata*) produces lift when the body is moving horizontally at a steady vertical position.

Although the body form of sturgeon is superficially similar to that of sharks (Patterson, 1982; Lauder and Liem, 1983; Grande and Bemis, 1996), their swimming kinematics have been shown to be quite different (Webb, 1986; Long, 1995; Lauder, 2000). Both sharks and actinopterygians, such as sturgeon, possess a heterocercal tail, yet studies aimed at elucidating its function have concentrated almost exclusively on the former (Grove and Newell, 1936; Affleck, 1950; Bainbridge, 1961; Alexander, 1965; Aleev, 1969; Simons, 1970; Thomson, 1976; Ferry and Lauder, 1996). Despite the fact that one of the major trends in the evolution of Osteichthyes is the origin of the homocercal tail from the plesiomorphic heterocercal condition, only a few researchers have examined the function of the heterocercal tail in basal actinopterygians (Alexander, 1966; Aleev, 1969; Lauder, 2000). The few studies that have experimentally determined the function of the heterocercal tail in sturgeon have produced conflicting results indicating that the sturgeon tail both does produce lift

(Alexander, 1966; Aleev, 1969) and does not produce lift (Lauder, 2000). These experiments involved the use of severed sturgeon tails, wooden models and three-dimensional kinematic analyses, all relatively indirect approaches for measuring the direction of force produced by the tail of a sturgeon swimming steadily forwards in the horizontal plane. No functional analysis has yet been attempted by directly measuring the orientation of force produced by the tail in a freely swimming sturgeon.

In addition, since fishes reside in a three-dimensional environment and commonly maneuver vertically in the water column (e.g. Hughes and Kelly, 1996; Webb et al., 1996; Gerstner, 1999; Wilga and Lauder, 1999), investigations that look only at horizontal swimming may fail to document the potential diversity of heterocercal tail function. There is no *a priori* reason to assume that the function of the heterocercal tail during horizontal locomotion is maintained when fishes rise or sink through the water column.

In this study, we examine the function of the heterocercal tail of a plesiomorphic ray-finned fish, the white sturgeon (*Acipenser transmontanus*), by measuring the direction of force produced by the tail over a range of natural swimming behaviors. In the past, force balance diagrams have been challenging to construct for freely swimming fishes because it is difficult to quantify the mean direction of force produced by the tail and, consequently, the direction of the associated reaction force. For example, to determine whether the tail generates a reaction force directed through the center of mass during locomotion, the direction of the mean vortex jet force generated by the tail must be estimated, and the center of mass and the angle of the body relative to the horizontal must be determined. Digital particle image velocimetry (DPIV) is a technique that enables direct measurement of the wake produced by the fins of freely swimming fish (Müller et al., 1997; Drucker and Lauder, 1999; Lauder, 2000). In previous DPIV analyses of the wake of the homocercal tail in teleost fishes (Müller et al., 1997; Wolfgang et al., 1999; Müller et al., 2000), the nature of the vortex ring structure of the wake has been demonstrated and quantified in the horizontal plane. Because we were interested in the role of the tail during holding and vertical maneuvering, and since sturgeon swim with the body at a significant angle to the horizontal plane (Wilga and Lauder, 1999), we focused our analysis of the wake on the vertical plane.

The specific goals of this study were to apply DPIV to the wake behind freely swimming sturgeon (i) to determine the direction of the force produced by the tail (and hence the direction of the reaction force) during steady horizontal swimming, (ii) to compare tail function during horizontal swimming with that during vertical maneuvering (rising, sinking), and (iii) to propose a new lift force and rotational balance diagram for sturgeon by integrating reaction force data on the tail with previous data from the pectoral fins.

## Materials and methods

### *Animals*

We obtained juvenile white sturgeon (*Acipenser transmontanus* Richardson) from commercial dealers in northern California. Sturgeon were individually housed in 20 l aquaria maintained at 20±1 °C and fed commercial fish pellets twice a week. Five sturgeon (25–31 cm total body length, $L$) were selected from among 13 for their ability to swim steadily in a flow tank. Sturgeon were trained to hold speed in a flow tank a few days prior to experimentation.

### *Digital particle image velocimetry and high-speed video recording*

Digital particle image velocimetry (DPIV) was employed to quantify the hydrodynamic characteristics of the wake produced by sturgeon swimming at two speeds, $1.2\,L\,s^{-1}$ and $2.0\,L\,s^{-1}$. Although analyses of the wake were carried out for the two swimming speeds to document changes in wake morphology as a function of speed, this paper will focus on data obtained for sturgeon swimming at $1.2\,L\,s^{-1}$. Sturgeon swim and maneuver readily at this speed, which is well within the range of speeds exhibited during locomotion, and the use of this speed allows for comparisons with previous studies of pectoral fin function (Wilga and Lauder, 1999). In addition, we found that wake structure is more amenable to force balance analysis at $1.2\,L\,s^{-1}$ than at $2.0\,L\,s^{-1}$ because of the shedding of discrete vortex rings.

A 600 l freshwater recirculating flow tank (working section 28 cm×28 cm×80 cm) maintained at 20±2 °C was seeded with 6 g of near-neutrally buoyant silver-coated glass spheres (mean diameter 12 μm, density $1.3\,g\,cm^{-3}$), which in turn were illuminated by a light sheet (10 cm×8 cm×0.1 cm) created by a Coherent 5 W argon/ion laser as in previous studies (Drucker and Lauder, 1999, 2000; Wilga and Lauder, 1999, 2000; Lauder, 2000). The light sheet was oriented in both the vertical and horizontal planes during separate experiments using a front-surface mirror to describe the wake (see Discussion in Drucker and Lauder, 1999, 2000; Wilga and Lauder, 1999; Lauder, 2000). Orthogonal orientations of the light sheet allowed for three-dimensional analysis and subsequent reconstruction of the wake although, for the purposes of measuring the direction of lift forces in this study, we found it necessary to analyze data from the vertical light sheet only. Lateral forces that arise from tail beats are measured using a horizontal light sheet, but these forces cancel during steady horizontal locomotion (e.g. Müller et al., 1997; Wolfgang et al., 1999). In contrast, vertical forces generated by the tail are not necessarily symmetrical about the horizontal plane and need to be directly measured to determine whether tail function is asymmetrical, taking into account that fish may swim with their body at a significant angle to the flow (Videler, 1993; Lauder, 2000). We used data from the horizontal light sheet as an adjunct to our more detailed analysis of the vertical light sheet data to confirm that the toroidal structure of the vortex rings produced by the tail during locomotion is similar to that described for fishes with homocercal tails (Müller et al., 1997, 2000; Wolfgang et al., 1999; Lauder, 2000).

DPIV software allowed us to reconstruct the orientation of the vortex rings shed by the tail. Two-frame cross-correlation

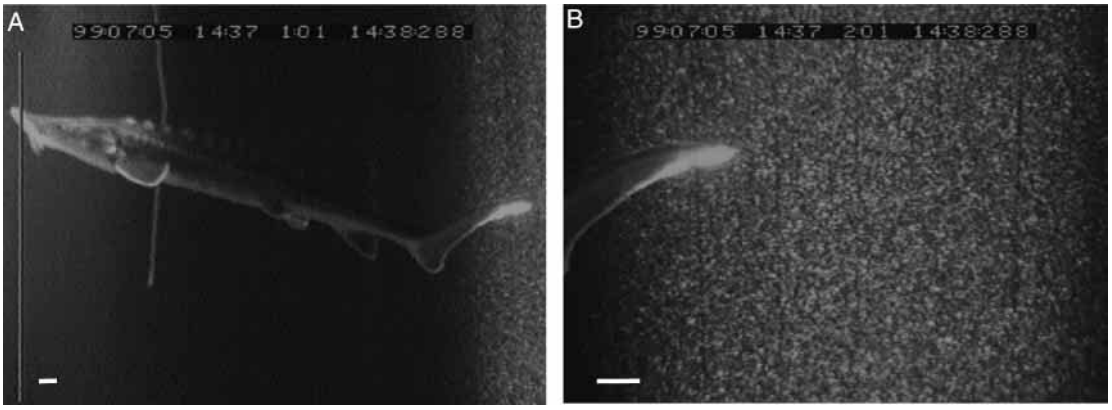


Fig. 1. Synchronized views from two high-speed video cameras illustrating lateral views of a sturgeon (*Acipenser transmontanus*) exhibiting steady horizontal locomotion (A) showing the body angle and position relative to the vertical laser sheet (note the positive body angle relative to the horizontal flow) and the lateral view of the vertical laser sheet (B) with illuminated tail and particles. The vertical object behind the sturgeon in A is a thin wire probe that was used as a physical and visual stimulus to guide the sturgeon into the middle of the flow tank and is positioned well behind the body of the sturgeon (>12 cm). The white scale bar in the lower left-hand corner of each image represents 1 cm.

analysis yielded a 20×20 matrix of 400 uniformly distributed velocity vectors (Insight version 3.0 software, TSI Inc., St Paul, MN, USA). The resultant two-dimensional velocity vector field, covering an area of approximately 8 cm×10 cm, was superimposed onto a plot of angular momentum to reveal the centers of vorticity for each vortex ring. Details of the analytical procedures have been presented in previous papers (Drucker and Lauder, 1999, 2000; Wilga and Lauder, 1999, 2000; Lauder, 2000).

Two electronically synchronized NAC HSV-500 high-speed video cameras filming at 250 frames $s^{-1}$ recorded images of the swimming sturgeon and the resultant wake directly downstream from the tail. Camera 1 provided a lateral view of the swimming sturgeon to record the body angle and path of motion, while camera 2 was positioned perpendicular to the light sheet to record the movement of the particles in the wake of the oscillating caudal fin (Fig. 1). Overlapping the two camera views allowed us to categorize the three swimming behaviors and to image the body angle while simultaneously capturing images of particle displacement created by the tail (Fig. 1). This method enabled us to identify discrete vortex rings being shed by a specific tail beat during a particular swimming behavior and to correlate wake morphology with body orientation and velocity at the same instant in time. Since the vertical light sheet was located in the center of the flow tank, tail beats that intersected the light sheet necessarily occurred well away from the surrounding walls.

### *Categorizing behaviors*

We quantified three swimming behaviors for sturgeon in the flow tank. These behaviors were similar to those observed by Wilga and Lauder (1999): rising through the water column, maintaining horizontal position in the water column (holding vertical position) and sinking through the water column. A tail beat was assigned to a rising behavior if the body experienced a positive vertical displacement while maintaining a steady horizontal position. Holding behavior was defined as a swimming sequence in which the fish exhibited no vertical or horizontal displacement. Sinking behavior occurred when the body experienced a negative vertical displacement while maintaining a steady horizontal position. Only sequences in which the tail was beating symmetrically (lateral excursions of equal magnitude) through the light sheet centered in the middle of the working section of the flow tank were considered for analysis. All sequences for all behaviors analyzed were selected on the basis of the criterion that sturgeon matched their speed with the flow and thus held their horizontal position without drifting downstream or accelerating upstream. Any sequences in which the sturgeon were turning to the right or left were excluded.

For rising and sinking behaviors, sequences were selected in which the sturgeon were maintaining a constant body angle while half-way through a rising or sinking event (i.e. not at the beginning of a rising or sinking event). We did this to quantify tail function during rising and sinking, but not during the transition from one swimming behavior to another. These criteria for choosing video sequences were the same as those used previously for the analysis of pectoral fin function (Wilga and Lauder, 1999). Considerable natural variation in the three swimming behaviors (rising, holding and sinking) provided a wide range of body angles over which to examine wake structure. This natural range of body angles and maneuvering velocities was extremely useful in assessing differences in tail function. Hydrodynamic variables quantified from the wake (see below) were plotted against this range of body angle values, which were distributed across the three types of behaviors. Although we provide mean values for each behavior to summarize the data (see Table 1), it is in fact the variation in body angles and maneuvering velocities that permits the quantitative assessment of caudal fin function as reflected in the graphs and regression analyses (see Figs 4–6). For each of

five fish, 3–5 trials for each of the three swimming behaviors were analyzed, generating a total of 62 tail-beat trials.

### *Variables*

Vertical velocities for rising and sinking behaviors were calculated by digitizing a fixed point on the body using a customized digitizing program at two known times and calculating the vertical distance covered in that time. Position data were unfiltered. Body angle (α) was defined as the angle between the horizontal and a line drawn between the anterior base of the insertion of the pectoral fin and the anterior base of the anal fin, which corresponds to the ventral surface of the body (Fig. 2A,B). The path of motion of the center of mass (β) was measured by connecting a line between two points digitized on the same part of the body (the anterior base of the pectoral fin) at two different times (200 ms apart). The angle of this line was then measured relative to the horizontal (Fig. 2A,B). The difference between the body angle and the path of motion of the center of mass is therefore the geometric angle of attack. Because we selected sequences in which sturgeon were swimming without rotating dorsally or ventrally, all points on the body travel parallel to the trajectory of the center of mass and, hence, the path of motion of the digitized point will be identical to that of the center of mass. The true center of mass did not have a natural visual marker and was experimentally determined *post-mortem* by iteratively balancing sturgeon between right and left side pins.

Ring axis angle (γ), defined as the angle between a line connecting the center of the two counter-rotating vortices of the vortex ring and the horizontal, was measured directly from analyzed images of the laser light sheet (Figs 2B, 3). Care was taken to analyze only vortex rings that were shed immediately downstream of the tail (between 1 and 5 cm downstream of the distal tip of the dorsal lobe) and to match individual body and hydrodynamic variables with the corresponding tail beat. Mean jet angle (δ) was calculated directly from the velocity vector field by averaging 8–12 high-velocity vectors located in the center of a vortex ring (Fig. 3).

### *Statistical tests*

A two-way, mixed-model analysis of variance (ANOVA) was conducted treating individual as the random effect and behavior as the fixed effect. A Bonferroni–Dunn *post-hoc* test was performed to determine whether differences among behaviors were significant at $P<0.01$. The $F$-value for the fixed effect of behavior was calculated as the mean square of the behavioral (fixed) effect divided by the two-way interaction term of the

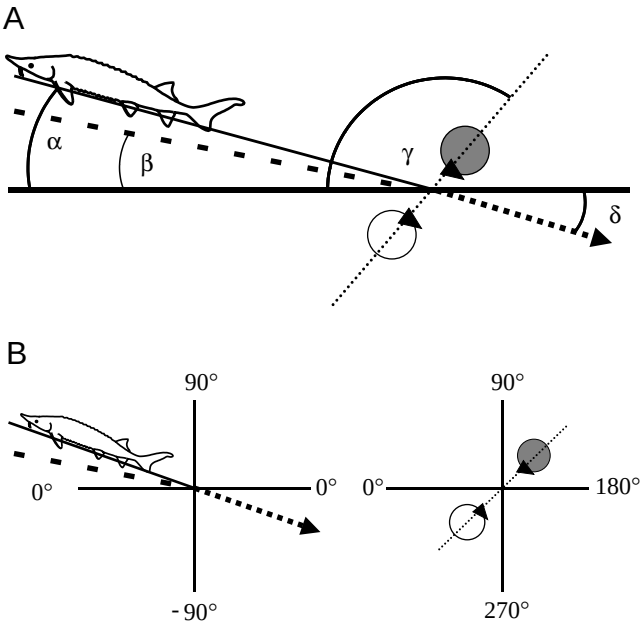


Fig. 2. (A) Diagram showing the four variables measured relative to horizontal: body angle (α), path of motion angle (β) depicted below the sturgeon for clarity, ring axis angle (γ) and mean jet angle (δ). Angle measurements are illustrated by the curved, solid lines. The dashed line represents the path of motion of the sturgeon. The path of motion and the body angle need not be the same and were measured separately. The dotted line connects the centers of two vortices in a vortex ring to define the ring axis, with the gray circle representing a counterclockwise center of vorticity and the white circle representing a clockwise center of vorticity. Mean jet flow is shown as a dotted arrow. For α, β and γ, any value above horizontal is considered positive and any value below horizontal is considered negative (B). For example, in this schematic diagram, α is +15 ° and β is +10 °, while δ is −15 °. Ring axis angle was measured out of 360 °, such that γ is +130 °.

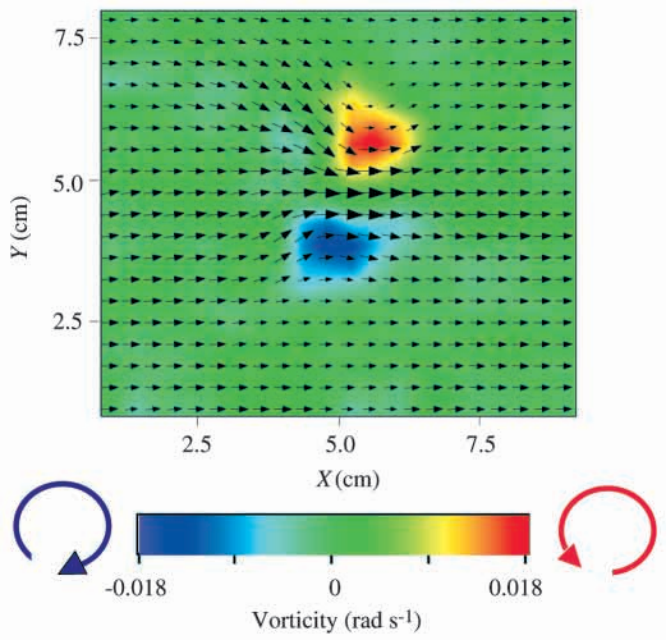


Fig. 3. Analyzed section of the vertical laser sheet in which black arrows represent a velocity vector field plotted over vorticity (magnitude and direction are represented in color). A jet of relatively strong flow, shown by the larger velocity vectors, passes between two counter-rotating vortices, where red represents a region of counterclockwise vorticity and blue represents a region of clockwise vorticity. The green area indicates regions of zero vorticity.

Table 1. *Summary statistics of DPIV variables in* Acipenser transmontanus *during three behaviors while swimming at 1.2* L $s^{-1}$

| Variable | Holding | Rising | Sinking | *P*-value | BD |
|---|---|---|---|---|---|
| Vertical body velocity (cm $s^{-1}$) | 0.02±1.1 | 4.1±1.9 | –5.4±1.4 | <0.001* | R>H>S |
| Body angle, α (degrees) | 7.4±1.9 | 13.6±1.9 | –5.5±3.5 | <0.001* | R>H>S |
| Path of motion angle, β (degrees) | 1.1±1.6 | 7.8±3.0 | –9.2±2.2 | <0.001* | R>H>S |
| Ring axis angle, γ (degrees) | 113.2±8.1 | 121.8±6.6 | 80.4±11.2 | <0.001* | H=R>S |
| Jet angle, δ (degrees) | –6.4±2.2 | –6.5±2.4 | 0.6±1.5 | <0.005* | H=R>S |

*Significant at the Bonferroni-corrected two-way ANOVA *P*-value of 0.01. Bonferroni–Dunn (BD) results: H, holding; R, rising; S, sinking. *L*, total body length.
Values are means ± S.E.M. (*N*=5).

random (individual) effect and the fixed effect. Results were Bonferroni-corrected for the five separate ANOVAs performed. Statistical tests were performed using Statview (version 4.5) for the Macintosh or calculated from Zar (1999).

Model I least-squares linear regression analyses were performed for the following pairs of dependent and independent variables, respectively: ring axis angle *versus* body angle, jet angle *versus* ring axis angle, jet angle *versus* body angle and jet angle *versus* path angle. The slopes from these experimental data were tested for significance and then compared statistically with the slope of the relationship expected (under our measurement conventions) if vortex ring jets were shed perpendicular to the vortex ring axis (expected slope 1) or if the vortex jet were parallel to the body axis (expected slope –1).

## Results

### *Body angle and wake variables*

Quantitative values for body and wake variables grouped by behavior are summarized in Table 1. Sturgeon adopt a positive body angle during rising and holding behaviors (13.6±1.9 ° and 7.4±1.9 °, respectively) and a negative body angle (–5.5±3.5 °) (means ± S.E.M., *N*=5) during sinking behaviors, which is a trend in accord with previous experiments (Wilga and Lauder, 1999). Body angle is not an acceptable surrogate for swimming trajectory, since the values for body angle during the three behaviors did not coincide with the values obtained for the path of motion angle (Table 1). For example, during holding behavior, the mean path of motion (1.1 °) was not significantly different from zero (horizontal), while the body was held at a mean angle of 7.4 °. Vertical displacement of the body during rising was of similar and opposite magnitude to that found for sinking, while very little vertical displacement occurred during holding behaviors.

Imaging the wake with vertical and horizontal light sheets reveals that after each tail beat a discrete vortex ring is shed with a jet of high-velocity flow through its center (Fig. 3). As body angle increased, ring axis angle increased (Fig. 4), maintaining a relationship that was significantly greater than 90 ° and significantly different from zero (slope of regression 1.30). However, the mean angle of the fluid jet through the center of the vortex ring decreased as ring axis angle increased (slope of regression –0.12) with a slope significantly greater than 90 ° and significantly different from zero (Fig. 5). Therefore, the mean jet angle is closer to horizontal than one

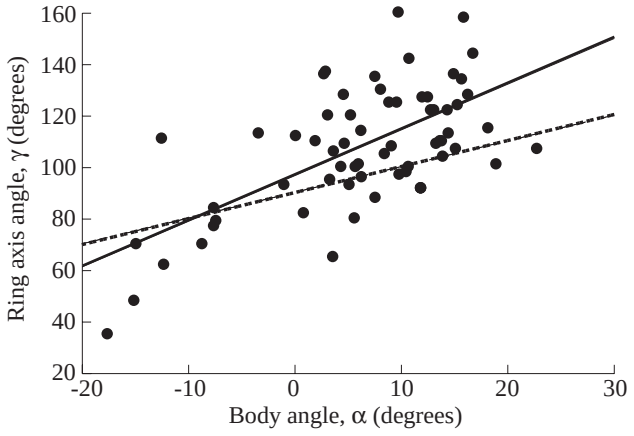


Fig. 4. Plot of ring axis angle (γ) *versus* body angle (α). The solid line is the significant linear regression relationship (*N*=62, *P*<0.0001, *r*=+0.66). The dashed line represents a perpendicular (90 °) relationship between ring axis angle and body angle. The slope of the regression is significantly greater than 90 °.

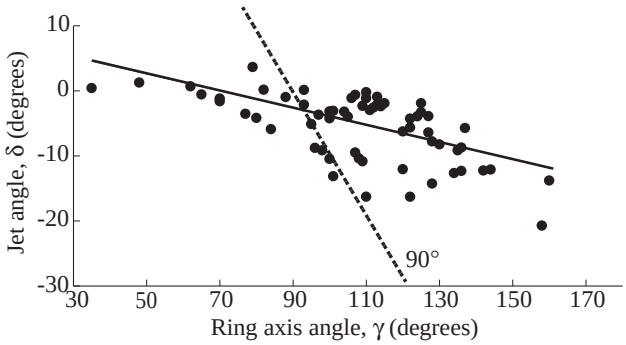


Fig. 5. Plot of jet angle (δ) *versus* ring axis angle (γ). The solid line is the significant linear regression for 62 data points (*P*<0.0001, *r*=–0.62). The dashed line represents a perpendicular (90 °) relationship between the fluid jet and the vortex ring axis. The slope of the regression is significantly less negative than the expected line and intersects the expected line, indicating that over a range of ring angles the jet angle is more horizontal than predicted.

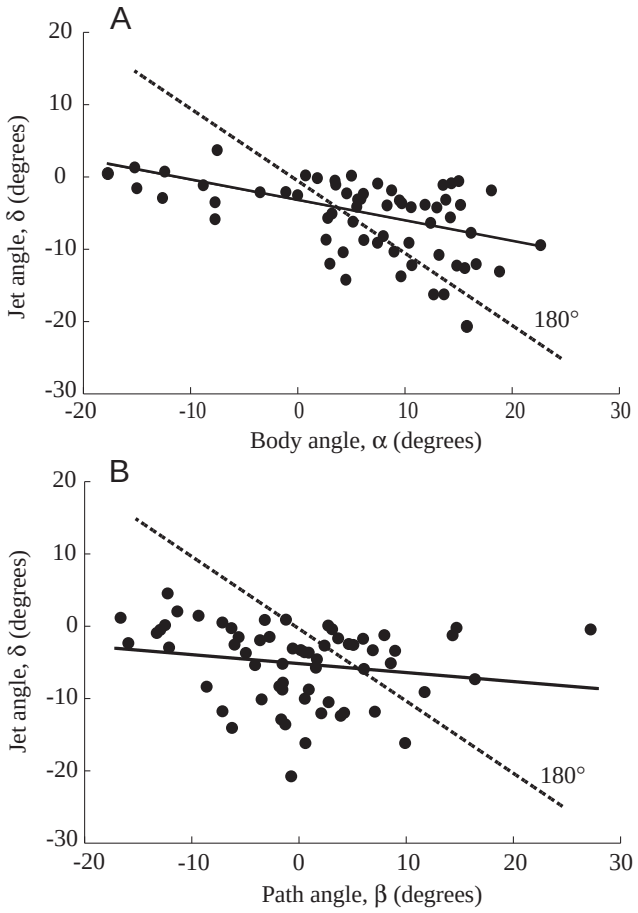


Fig. 6. (A) Plot of jet angle (δ) *versus* body angle (α). The solid line is the significant linear regression for 62 data points ($P$<0.0001, $r$=–0.50). The dashed line represents the 180° relationship that is expected if the fluid jet produced by the tail were parallel to the body angle. The slope of the regression is significantly less negative than the expected line. (B) Plot of jet angle (δ) *versus* path angle (β). The solid line is the linear regression for 62 data points, and the slope for this line is significantly different from the 180° line ($P$<0.0001, $r$=–0.19). Mean path angle values were approximately 4–6° less than mean body angle values for all behaviors.

would expect had its value changed at the same rate as the ring axis angle over the three swimming behaviors.

Vortex jet angle decreases (Fig. 6A) but at a significantly slower rate (slope of regression –0.28, $P$<0.0001) than expected if a parallel (180°) relationship was observed relative to body angle. Jet angles are closer to horizontal than one would expect if the value for jet angles and body angles (Fig. 6A) changed at the same rate. The result is that the range of jet angle values is much smaller than the associated range of body angles. When the mean jet angle (δ) is plotted against the mean path angle (β), as in Fig. 6B, the slope of the regression is –0.14, not significantly different from zero ($P$=0.09) and significantly different from the 180° expected relationship ($P$<0.0001). The values for path angle are approximately 4–6° more negative than the body angle values for each of the three associated behaviors, producing an overall left-ward shift of the data points.

Five separate Bonferroni-corrected ANOVAs revealed that there was significant variation in mean vertical body velocity, body angle (α), path angle (β), ring axis angle (γ) and jet angle (δ) among the three swimming behaviors (Table 1). Each behavior was significantly different from the others for body velocity, body angle (α) and path angle (β). While no significant differences were found for ring axis angle between rising and holding behaviors, both behaviors were significantly different from sinking behavior ($P$<0.001). Similarly, no significant differences were found for jet angle between rising and holding behaviors, but the mean jet angle values for both these behaviors were significantly different from the mean jet angle value for a sinking behavior ($P$<0.005).

## Discussion

### *Vortex wake structure of freely swimming sturgeon*

Although our study reveals that vortex rings shed by the heterocercal tail of white sturgeon are qualitatively similar in morphology to vortex rings shed by the homocercal tail of teleost fishes (Videler, 1993; Müller et al., 1997; Wolfgang et al., 1999; Lauder, 2000), the axes of the vortex rings produced by sturgeon are more oblique with respect to body angle (Figs 2, 4) than the vortex rings illustrated in vertical section in the wake of bluegill sunfish (*Lepomis macrochirus*) (Lauder, 2000). The conventions shown in Fig. 2 illustrate how the oblique axis of a shed vortex ring describes an obtuse angle (>90°) with the body angle. The relationship between ring axis angle (γ) and body angle (α) observed for sturgeon does not conform to the perpendicular relationship that might be expected if we assumed that fins can be modeled as rigid, plate-like control surfaces. For example, a sinking sturgeon with a body angle of –10° exhibits a ring axis angle of 85°, while a rising sturgeon with a body angle of +15° exhibits a ring axis angle of 120° (Fig. 4). The linear regression of ring axis on body angle is significantly different from the expected 90° relationship ($P$<0.01), suggesting that the tail is not well modeled as a flat plate. Lauder (2000) has contrasted the complex kinematics of the heterocercal sturgeon tail with the kinematics of the homocercal tail in bluegill sunfish. During the tail-beat cycle, the extreme flexibility of the posterior end of the dorsal lobe (resulting from the lack of structural integrity and intrinsic musculature) causes it to lag behind both the anterior part of the dorsal lobe and the ventral lobe (Lauder, 2000). This results in the posterior end of the dorsal lobe traveling in the opposite direction to the ventral lobe during much of the tail-beat cycle.

This kinematic pattern may be responsible for generating the inclined vortex rings produced in the wake of a swimming sturgeon, where the two centers of vorticity do not lie in a direct vertical line with each other such that one center of vorticity is located anterior or posterior to the other (Fig. 3). Tilted vortex rings may be created experimentally by using a piston to pulse a slug of fluid through a cylinder and out of the

orifice of an inclined nozzle (Webster and Longmire, 1996; Lim, 1998). The axes of these vortex rings tend to be slightly less inclined than the nozzle angle. By changing the amplitude and frequency of force-pulsing and altering nozzle geometry, asymmetries in the orientation and the shape of the vortex rings can be achieved. For instance, the diameter of vortex rings can be altered by changing the amount of fluid pulsed through the nozzle (Maxworthy, 1977; Webster and Longmire, 1996). In addition, the morphological and behavioral characteristics of vortex rings change as they progress downstream from the point of shedding. The magnitude of the vortex ring axis inclination increases with downstream distance (Webster and Longmire, 1996), and the two counter-rotating centers of vorticity spread apart from each other because of vortex stretching (Lim, 1998).

In the tilted vortex rings produced by inclined nozzles, the direction of the jet is nearly perpendicular to the ring axis (Webster and Longmire, 1996), which is inconsistent with what we have found for biologically tilted vortex rings produced by the sturgeon tail. Although the exact hydrodynamic mechanism by which sturgeon generate tilted rings has yet to be investigated, the longer dorsal lobe of the heterocercal tail may retain the bound vorticity of the developing vortex ring longer than the shorter ventral lobe and, thus, cause the tilted orientation of the shed vortex ring, much like the differential anterior–posterior surface lengths of a nozzle cut at an inclined angle. When sturgeon rise in the water column, the dorsal lobe of the tail is oriented more horizontally relative to the oncoming water flow than when they are holding vertical position. Webster and Longmire (1996) found that the relative increase in the inclination of the ring axis decreases with nozzle inclination. This may explain why sturgeon adopting higher body angles (and thus larger tail inclinations) produce ring axis angles that are relatively smaller than the ring axis angles observed for lower body angles.

The phenomenon of biologically tilted rings associated with heterocercal tail morphology remains to be documented in other basal actinopterygians and sharks. An analysis of a time-dependent developmental sequence of a vortex ring as it is created and shed by the tail, such as that accomplished by Drucker and Lauder (1999) for pectoral fins in bluegill sunfish, is needed before we are able to understand the mechanism responsible for establishing vortex ring axis orientation and the non-perpendicular relationship between ring axis angle and jet angle. Such an analysis will require a three-dimensional characterization of fluid velocity around the tail. Our data show that, instead of the jet flowing perpendicularly through the center of the vortex ring, the heterocercal tail of the sturgeon causes the jet to be angled more horizontally than expected over a range of ring axis angles. Work by Lauder (2000) shows that the vortex jet in rings shed by the homocercal tail of bluegill sunfish is also ventrally inclined, suggesting that even in homocercal tails the vortex jet need not be perpendicular to the ring axis.

Deviation from a consistent relationship between mean jet angle and mean body angle over the three swimming behaviors illustrates that sturgeon can actively alter the angle of mean jet flow produced by their tail during maneuvering (Fig. 6). For example, if the relationship between the vortex jet angle and body angle in swimming sturgeon was invariant, then the effectively equal and opposite magnitudes observed for these two variables during holding behavior (Table 1) would be maintained during rising and sinking behavior. In fact, during rising behavior, the vortex jet angle is the same as during holding behavior, despite the doubling of body angle. Similarly, during sinking, the jet angle is effectively zero while the body angle is nearly 6° below horizontal (Table 1). Sturgeon are capable of altering tail vortex jet angles by up to 10° and may be actively able to control the direction of force produced by their tail.

Dissected and cleared-and-stained specimens show very little musculature associated with the fin rays of the tail (Lauder, 1989), suggesting that sturgeon may control their tail actively by differential contraction of the epaxial and hypaxial musculature in the caudal region. Contraction of such body musculature may stiffen regions of the tail or tilt the tail up or down, thus altering the angle of the tail surface and hence the angle of the vortex jet.

### *Vertical force balance*

We propose a new vertical force diagram that uses the same general conventions as those of Wilga and Lauder (1999) but provides more detail now that we have measured the body angle, path of motion and direction of the reaction force produced by the tail during holding and vertical maneuvering. We separated the vertical forces generated by swimming sturgeon into four regions (Fig. 7A); the head and pectoral fins ($F_{H+P}$), which is anterior to the center of mass, the weight of the fish at the center of mass ($F_W$), the body posterior to the center of mass ($F_B$) and the tail ($F_T$). The red arrows in Fig. 7A show the orientations of these vertical forces. The presence of a red circle indicates that a region exhibits no vertical force contribution. The reaction force ($F_R$) experienced by the tail is equal but opposite in magnitude to the jet angle. The presence or absence of a vertical component of the reaction force at the tail ($F_T$) in the fish frame of reference is determined by comparing the direction of the reaction force (Fig. 7A, $F_R$) with the path of motion of the center of mass (dashed line) and not with the body angle (solid line).

The inclined body angle of a rising sturgeon (+14° above horizontal on average) causes oncoming water to generate an upward force acting on the ventral surface of the body both anterior and posterior to the center of mass (Fig. 7, rising). Wilga and Lauder (1999) have shown that the pectoral fins flip upwards to initiate a lift force at the beginning of a rise by altering the orientation of the head and the anterior region of the body. During a rise, lift forces are probably generated by the pectoral fins, the ventral surface of the head and the ventral surface of the body posterior to the center of mass (Fig. 7A, rising, $F_{H+P}$). During rising behavior, the tail generates a mean jet of −7° below horizontal (Fig. 7A), indicating that there is very little vertical force component (lift) produced by the tail ($F_T$) because the reaction force ($F_R$) is effectively in line with the path of motion of the center of mass (8°). Lift forces

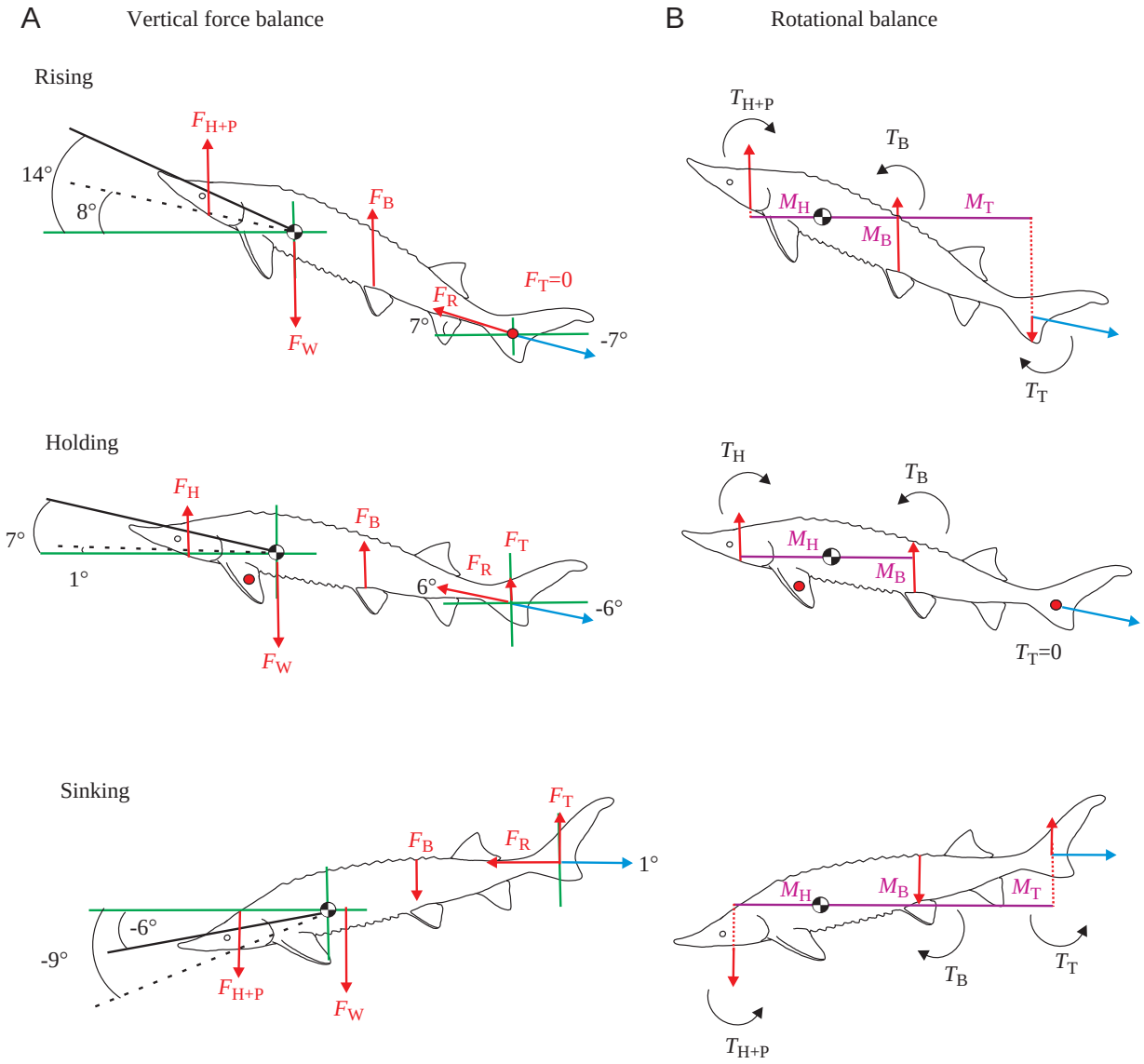


Fig. 7. Vertical force balance diagrams (A) and rotational balance diagrams (B) for sturgeon exhibiting three different behaviors: rising, holding and sinking. Blue arrows represent mean jet flow through the vortex rings shed by the tail, black-and-white checkered circles represent the center of mass, green lines represent the *X* and *Y* axes for reference, red arrows indicate the presence of vertical forces, purple lines represent the moment arm, red circles indicate no vertical force contribution, solid black lines represent the body angle of the fish, dashed black lines represent the path of motion of the center of mass and curved black arrows represent the direction of torque. Jet angles, body angles and path angles are based on experimental data obtained from this study. $F_{H+P}$ is the positive vertical component of the reaction force experienced by the head and pectoral fins when water impacts the ventral surface, $F_W$ is the downward vertical force due to the weight of the negatively buoyant sturgeon, $F_B$ is the upward vertical force component created by water impacting the ventral surface of the body, $F_R$ is the reaction force produced by the tail and $F_T$ (when present) is the vertical component of $F_R$. During rising behavior, there is no $F_T$ because $F_R$ is effectively in line with the path of motion of the fish. For both holding and sinking behaviors, $F_T$ results from $F_R$ not being in line with the path of motion. Torque is given by force (red arrow) multiplied by moment arm (purple line). The tail experiences no torque during holding behavior because there is no perpendicular force (represented by a red circle) acting on the moment arm since the reaction force passes through the center of mass. $T_{H+P}$, torque on the head and pectoral fins; $T_B$, torque on the body; $T_T$, torque on the tail; $M_H$, moment arm on the head; $M_B$, moment arm on the body; $M_T$, moment arm on the tail.

generated by the positive angle of attack of the ventral body surface anterior and posterior to the center of mass are greater than the force generated by the weight of the fish ($F_W$). This inequality of vertical forces causes the sturgeon to rise up through the water column (Fig. 7A, rising; Table 1).

The body of a sturgeon holding vertical position is inclined at an average angle of +7° above horizontal, generating lift forces along the body similar to those of a rising sturgeon, but presumably with less magnitude because of the smaller body angle (Fig. 7A, holding). However, the mean jet angle produced

by the tail is –6° on average, producing a reaction force (+6°) that is not parallel to the path of motion (+1° on average and not significantly different from 0°). This results in the production of a positive vertical force by the tail ($F_T$) relative to the path of motion of the center of mass. Positive lift forces generated by the inclined ventral body surface and tail are balanced by the force due to the weight of the fish, causing the sturgeon to maintain its vertical position in the water column. Electromyography combined with DPIV analysis has shown that sturgeon pectoral fins provide negligible lift while holding vertical position (Wilga and Lauder, 1999).

During sinking behavior, the dorsal surface of the body is negatively inclined (–6° on average), causing reaction forces along the body of the sturgeon to be directed downwards (Fig. 7A, sinking). Body surface forces act in the same direction as the weight of the fish, causing a high downward velocity. This high downward velocity is caused both by the relatively larger lift force produced by the tail ($F_T$) and by the larger downward force documented by Wilga and Lauder (1999) for the pectoral fins. The tail produces a jet that is effectively horizontal in direction (+1° on average). When the $F_R$ associated with the mean jet angle is compared with the path of motion of the sinking sturgeon (–9° on average), the tail experiences a force ($F_T$) directed upwards relative to the path of motion of the center of mass.

Because vertical forces are either in balance (steady horizontal locomotion) or not in balance (rising or sinking), the relationship among the forces along the body changes with behavior. The current vertical force balance diagram for holding, rising and sinking sturgeon set forth by Wilga and Lauder (1999) assumes that the reaction force experienced by the tail passes near the center of mass. This generalization is supported by the data in the present study for sturgeon holding vertical position, but not for sturgeon that are rising or sinking.

### *Rotational balance*

Previous research has shown that the pectoral fins of swimming sturgeon produce a vertical force contribution during rising or sinking, but not while holding vertical position (Wilga and Lauder, 1999). In addition, it is the movement of the pectoral fins that is responsible for initiating rising or sinking behavior (Wilga and Lauder, 1999) by rotating the body around the center of mass. Therefore, at the beginning of rising or sinking behavior, the body of the sturgeon is not in rotational equilibrium. A lateral view of the left side of the sturgeon (Fig. 7, holding) illustrates that the body must rotate clockwise to rise and counterclockwise to sink. Our data on rising or sinking behavior were obtained after the initiation of rising or sinking so that rotational equilibrium had been reached and the sturgeon was moving with a constant body angle up or down through the water column. For the rotational balance diagram illustrated in Fig. 7B, the presence (red arrow) or absence (red circle) of a vertical force component contributing to the moment about the tail is obtained by comparing the direction of the reaction force ($F_R$; not illustrated in Fig. 7B but shown in Fig. 7A) with the position of the center of mass, which lies along the body angle. A positive vertical component of the reaction force relative to the path of motion can actually make a negligible contribution to the rotational moment of the fish if this force is being directed through the center of mass. This is seen when a holding sturgeon in the vertical force balance column is compared with a holding sturgeon in the rotational balance column: the tail generates a positive vertical force because the angle of the reaction force is 5° greater than the path of motion (Fig. 7A, holding), but this reaction force is in line with the center of mass (no rotational moment; Fig. 7B, holding).

During rising behavior (Fig. 7B, rising), a clockwise torque (curved black arrow) is generated at the tail of the sturgeon ($T_T$). The tail experiences a negative vertical force because the reaction force (+7°) passes ventral to the center of mass (body angle +14°). The tail experiences a clockwise torque ($T_T$) resulting from the vertical force component of $F_R$ multiplied by the moment arm, $M_T$, shown as a purple line. Flow coming into contact with the upwardly inclined body generates a clockwise torque at the head and pectoral fins ($T_{H+P}$) and a counterclockwise torque at the region of the body posterior to the center of mass ($T_B$). The overall rotation of the body is zero since sturgeon are observed rising at a constant body angle. Thus, the clockwise rotation produced in the region of the head and pectoral fins and the clockwise rotation produced at the tail are balanced by the counterclockwise torque produced by the body ($T_{H+P}+T_T=T_B$).

During holding behavior (Fig. 7B, holding), there is no torque resulting from the tail ($T_T=0$) because the direction of the reaction force (+6°) is effectively in line with the center of mass (+7°). A clockwise torque is produced by the head ($T_H$) but not by the pectoral fins because the pectoral fins do not produce lift during holding behavior. This clockwise torque must be canceled out by the counterclockwise rotation of the region of the body posterior to the center of mass ($T_B$), since sturgeon are observed to swim at a constant body angle ($T_H=T_B$).

During sinking behavior (Fig. 7B, sinking), there is a counterclockwise torque originating at the head and pectoral fins ($T_{H+P}$), a clockwise rotation about the posterior end of the body ($T_B$) originating from flow coming into contact with the downwardly inclined dorsal body surface and a counterclockwise rotation about the tail ($T_T$) resulting from the mean tail reaction force (1°) passing dorsal to the center of mass. The overall rotation of the body is zero since sturgeon were observed sinking at a constant body angle. The counterclockwise torque produced by the head and pectoral fins and the counterclockwise torque generated by the tail are balanced by the clockwise torque produced by the body ($T_{H+P}+T_T=T_B$).

### *Concluding remarks and future directions*

Our overall aim in this study was to quantify the direction of force production by the heterocercal tail of sturgeon in the vertical plane during both steady horizontal locomotion and vertical maneuvering. Heterocercal tail function proves to be more complex than previously thought when examined over a range of vertical maneuvering behaviors using quantitative

flow visualization. While both kinematic analysis of the tail of sturgeon swimming horizontally (Lauder, 2000) and force balance diagrams based on data from sturgeon pectoral fins (Wilga and Lauder, 1999) suggest that the tail produces a reaction force that is in line with the center of mass, DPIV analysis of the tail for sturgeon swimming horizontally indicates that, even though the reaction force passes through the center of mass during horizontal locomotion, a lift force is produced, as predicted from data on heterocercal tail function in sharks (Ferry and Lauder, 1996).

Although we have proposed a hypothesis for force and rotational balance and contributed quantitative information on the direction of the tail reaction forces relative to the center of mass and its path of motion, the magnitudes of the forces generated at various points along the body remain to be measured. Quantifying the magnitude of fluid forces on the body surface would allow comparison between the force balance diagram of a basal ray-finned fish and a teleost fish (e.g. Drucker and Lauder, 1999) and provide the first *in vivo* quantitative force balance on a fish swimming with caudal fin propulsion. In addition, tracking the change in these forces during the transition between holding, rising and sinking would offer further insight into the mechanisms by which vertical maneuvering is achieved.

We acknowledge Jen Nauen, Eliot Drucker, and Cheryl Wilga for their invaluable assistance in analysis and helpful discussions throughout the project. We would also like to thank Eric Tytell for pointing out a useful reference. Support was provided by NSF grant (IBN-9807012) to G.V.L.

## References

**Affleck, R. J.** (1950). Some points in the function, development and evolution of the tail in fishes. *Proc. Zool. Soc. Lond.* **120**, 349–368.

**Aleev, Y. G.** (1969). *Function and Gross Morphology in Fish* (translated from the Russian by M. Raveh). Jerusalem: Keter Press.

**Alexander, R. McN.** (1965). The lift produced by the heterocercal tails of Selachii. *J. Exp. Biol.* **43**, 131–138.

**Alexander, R. McN.** (1966). Lift produced by the heterocercal tail of *Acipenser*. *Nature* **210**, 1049–1050.

**Bainbridge, R.** (1961). Problems of fish locomotion. *Symp. Zool. Soc. Lond.* **5**, 13–32.

**Drucker, E. G. and Lauder, G. V.** (1999). Locomotor forces on a swimming fish: three-dimensional vortex wake dynamics quantified using digital particle image velocimetry. *J. Exp. Biol.* **202**, 2393–2412.

**Drucker, E. G. and Lauder, G. V.** (2000). A hydrodynamic analysis of fish swimming speed: wake structure and locomotor force in slow and fast labriform swimmers. *J. Exp. Biol.* **203**, 2379–2393.

**Ferry, L. A. and Lauder, G. V.** (1996). Heterocercal tail function in leopard sharks: a three-dimensional kinematic analysis of two models. *J. Exp. Biol.* **199**, 2253–2268.

**Gerstner, C. L.** (1999). Maneuverability of four species of coral-reef fish that differ in body and pectoral-fin morphology. *Can. J. Zool.* **77**, 1102–1110.

**Grande, L. and Bemis, W. E.** (1996). Interrelationships of Acipenseriformes, with comments on 'Chondrostei'. In *Interrelationships of Fishes* (ed. M. Stiassny, L. Parenti and G. D. Johnson), pp. 85–115. San Diego: Academic Press.

**Grove, A. J. and Newell, G. E.** (1936). A mechanical investigation into the effectual action of the caudal fin of some aquatic chordates. *Ann. Mag. Nat. Hist.* **17**, 280–290.

**Hughes, N. F. and Kelly, L. H.** (1996). A hydrodynamic model for estimating the energetic cost of swimming maneuvers from a description of their geometry and dynamics. *Can. J. Fish. Aquat. Sci.* **53**, 2484–2493.

**Lauder, G. V.** (1989). Caudal fin locomotion in ray-finned fishes: historical and functional analyses. *Am. Zool.* **29**, 85–102.

**Lauder, G. V.** (2000). Function of the caudal fin during locomotion in fishes: kinematics, flow visualization and evolutionary patterns. *Am. Zool.* **40**, 101–122.

**Lauder, G. V. and Liem, K. F.** (1983). The evolution and interrelationships of the actinopterygian fishes. *Bull. Mus. Comp. Zool.* **150**, 95–197.

**Lim, T. T.** (1998). On the breakdown of vortex rings from inclined nozzles. *Phys. Fluids* **10**, 1666–1671.

**Long, J. H.** (1995). Morphology, mechanics and locomotion: the relation between the notochord and swimming motions in sturgeon. *Env. Biol. Fish.* **44**, 199–211.

**Maxworthy, T.** (1977). Some experimental studies of vortex rings. *J. Fluid Mech.* **81**, 465–495.

**Müller, U. K., Stamhuis, E. J. and Videler, J. J.** (2000). Hydrodynamics of unsteady fish swimming and the effects of body size: comparing the flow fields of fish larvae and adults. *J. Exp. Biol.* **203**, 193–206.

**Müller, U. K., Van den Heuvel, B., Stamhuis, E. J. and Videler, J. J.** (1997). Fish foot prints: morphology and energetics of the wake behind a continuously swimming mullet (*Chelon labrosus* Risso). *J. Exp. Biol.* **200**, 2893–2906.

**Olson, E. C.** (1971). *Vertebrate Paleozoology*. New York: John Wiley.

**Patterson, C.** (1982). Morphology and interrelationships of primitive actinopterygian fishes. *Am. Zool.* **22**, 241–259.

**Simons, J. R.** (1970). The direction of the thrust produced by the heterocercal tails of two dissimilar elasmobranchs: the Port Jackson shark, *Heterodontus portusjacksoni* (Meyer) and the piked dogfish, *Squalus megalops* (Macleay). *J. Exp. Biol.* **52**, 95–107.

**Thomson, K. S.** (1976). On the heterocercal tail in sharks. *Paleobiol.* **2**, 19–38.

**Videler, J. J.** (1993). *Fish Swimming*. New York: Chapman & Hall.

**Webb, P. W.** (1986). Kinematics of lake sturgeon, *Acipenser fulvescens*, at cruising speeds. *Can. J. Zool.* **64**, 2137–2141.

**Webb, P. W., Laliberte, G. D. and Schrank, A. J.** (1996). Does body and fin form affect the maneuverability of fish traversing vertical and horizontal slits? *Env. Biol. Fish.* **46**, 7–14.

**Webster, D. R. and Longmire, E. K.** (1996). Vortex dynamics in jets from inclined nozzles. *Phys. Fluids* **9**, 655–666.

**Wilga, C. D. and Lauder, G. V.** (1999). Locomotion in sturgeon: function of the pectoral fins. *J. Exp. Biol.* **202**, 2413–2432.

**Wilga, C. D. and Lauder, G. V.** (2000). Three-dimensional kinematics and wake structure of the pectoral fins during locomotion in leopard sharks, *Triakis semifasciata*. *J. Exp. Biol.* **203**, 2261–2278.

**Wolfgang, M. J., Anderson, J. M., Grosenbaugh, M. A., Yue, D. K. P. and Triantafyllou, M. S.** (1999). Near-body flow dynamics in swimming fish. *J. Exp. Biol.* **202**, 2303–2327.

**Zar, J. H.** (1999). *Biostatistical Analysis*, fourth edition. Upper Saddle River, NJ: Prentice Hall.